nature methods

Review article

https://doi.org/10.1038/s41592-025-02890-1

Selecting the optimal cell migration assay: fundamentals and practical guidelines

Received: 22 December 2024

Accepted: 13 August 2025

Published online: 18 December 2025

Check for updates

Wenxuan Du[1,2], Praful R. Nair[2], Andre Forjaz[1,2], Jude M. Phillip[1,2,3,4,5] ✉, Pei-Hsun Wu[1,2] ✉ & Denis Wirtz[1,2,5,6] ✉

Cell migration is a key cellular process that drives major developmental programs. To mimic and mechanistically understand cell migration in these different contexts, different assays have been developed. However, owing to the lack of practical guidelines, these different cell migration assays are often used interchangeably. This and the inherent dynamic nature of cell migration, which often requires sophisticated live-cell microscopy, may have caused cell migration to be notably less well understood than equally important cell functions, such as cell differentiation or proliferation. In this Review, we describe commonly used custom and commercial in vitro and in vivo cell migration assays and provide a comprehensive practical guide and decision tree outlining how to choose and implement an assay that best suits the biological question at hand. We hope this guidance spurs biological insights into this complex process and encourages future methods development.

Migration is a key cellular process that drives major developmental programs including gastrulation and blood vessel sprouting[1,2], promotes tissue repair and regeneration[3] and catalyzes disease progression, including immune infiltration in tissues and metastatic spread in cancer[4,5] (Supplementary Fig. 1). Depending on the microenvironmental context, cells can undergo distinct modes of migration. For instance, cells can migrate collectively, for which intercellular contact is maintained, as small clusters or individual entities[6,7], randomly or in a directed fashion[5,8] (Supplementary Fig. 2). Cell migration can be directionally biased by the application of external biochemical[5] (chemotaxis), mechanical[9,10] (durotaxis), electric[11,12] (galvanotaxis) or magnetic field[13] (magnetotaxis) gradients produced by neighboring cells or the extracellular matrix (ECM; Supplementary Fig. 3). Depending on the extracellular context, cells can also migrate along linear one-dimensional (1D) tracks (for example, confined migration guided by collagen fibers), on relatively flat (two-dimensional (2D)) surfaces (for example, collective migration of epithelial sheets), in three dimensions (for example, cancer cells migrating through the three-dimensional (3D) stromal matrix) and even in 2.5 dimensions (2.5D; for example, transformed cells of an epithelial sheet moving through the basement membrane; Supplementary Fig. 4).

The same cells can adopt different modes and molecular mechanisms of migration, as they move through different types of microenvironment. For instance, cancer cells in a 3D stromal collagen-rich matrix will typically adopt a mesenchymal mode of migration (for which the front edge grows and attaches to the ECM, while the rear edge detaches for net motion) driven by thin dendritic protrusions formed dynamically via actin filament assembly and myosin II-based contractility[14–17]. The same cells locally confined by collagen fibers may move as clusters and use dynamic water intake and propulsion to move forward[18,19]. By contrast, amoeboid cells such as T cells will dynamically produce actin-rich pseudopods, hydrostatically generated blebs (a type of protrusion where the plasma membrane temporarily detaches from the underlying cytoskeleton) and a highly contractile protrusion at the rear (uropod) to migrate[20,21]. Cells, especially cancer cells, may switch dynamically between these different types

[1]Department of Chemical & Biomolecular Engineering, Johns Hopkins University, Baltimore, MD, USA. [2]Institute for NanoBioTechnology, Johns Hopkins University, Baltimore, MD, USA. [3]Department of Biomedical Engineering, Johns Hopkins University, Baltimore, MD, USA. [4]Translational Therapeutics and Regenerative Engineering Center, Johns Hopkins University, Baltimore, MD, USA. [5]Department of Oncology, Johns Hopkins School of Medicine, Johns Hopkins University, Baltimore, MD, USA. [6]Department of Pathology, Johns Hopkins School of Medicine, Johns Hopkins University, Baltimore, MD, USA. ✉e-mail: jphillip@jhu.edu; pwu@jhu.edu; wirtz@jhu.edu

https://doi.org/10.1038/s41592-025-02890-1

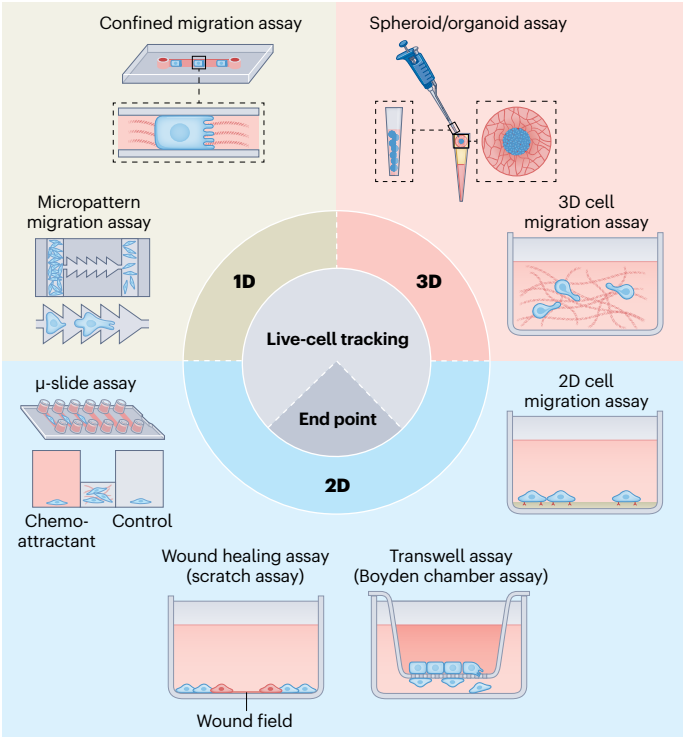

Fig. 1 | Commonly used commercial and custom in vitro cell migration assays. These assays are categorized according to the 'dimensionality' of the assays (1D, 2D or 3D) and the type of data acquisition (end-point measurement or live-cell tracking). Figure created in BioRender.com. Du, F. (2025) https://BioRender.com/ih4u4w3.

of migration, as they face topologically and biochemically different milieus during metastatic spread[22–24]. Accordingly, cells may adopt different biophysical and biomolecular mechanisms of force generation and adhesion to adapt their migration phenotype to their extracellular environment (Supplementary Fig. 5).

The onset of migration of otherwise stationary cells can be prompted by extracellular triggers, such as a global change in the concentration of cytokines in the cellular milieu caused by other cells (for example, paracrine signaling-triggered onset of cell migration)[5], a local change in local cell density induced by cell proliferation (for example, autocrine signaling-based onset of migration)[25,26] or following genetic or epigenetic cell transformation (for example, epithelium–mesenchymal transition in development and cancer)[27,28].

To mimic and mechanistically understand cell migration in these different contexts, a plethora of custom and commercial in vitro assays have been developed (Fig. 1). Although they provide ease of use, most commercial assays (for example, the Transwell assay) only provide end-point measurements that are proxies of migration. This precludes single-cell analysis, as the identity of individual cells is lost during the experiments and renders impossible the computation of important migration parameters such as cell diffusivity and persistence of migration. Moreover, these commercial assays do not provide the versatility required to mimic the different architecture and composition of the local microenvironments encountered, for instance, by cancer cells along the metastatic cascade (Supplementary Fig. 1). Vice versa, although custom cell migration assays allow to more closely mimic cell migration in vivo and more sophisticated post-experimental analysis, they are harder to implement and are low throughput (Table 1).

Below, we describe ten commercial and custom cell migration in vitro assays and two in vivo assays. More assays have been described in the literature, but we focus on the more widely used cell migration assays. These assays are split into two major categories: in vitro versus in vivo cell migration assays. The in vitro assays consist of the wound healing assay (scratch assay; Fig. 2), the Transwell assay (Boyden chamber assay; Fig. 3), the 2D/3D cell migration assay (single-cell migration assay; Fig. 4), the spheroid/organoid invasion assay (Fig. 5), the μ-slide chemotaxis assay (Supplementary Fig. 6), the confined cell migration assay (Supplementary Fig. 7) and the micropatterned migration assay (Supplementary Fig. 8). Based on the different classification criteria summarized above, these in vitro assays can be further categorized by the dimensionality of the migration to be studied (1D versus 2D or 3D) and the type of data acquisition desired (live-cell versus end-point measurements; Fig. 1). The in vivo assays consist of multi-photon microscopy and light-sheet microscopy. For each in vitro assay, we provide an explanatory cartoon, as well as information about: (1) the dimensionality of the assay (Supplementary Fig. 4); (2) the ease/difficulty of implementation; (3) the cost; (4) a commercial source, if it exists; (5) the productive capacity, that is, the number of cell conditions that can be probed simultaneously; (6) the necessity of a live-cell microscope to run the assay; (7) the possibility to perform post-assay downstream molecular analysis, such as western blotting or single-cell RNA sequencing (RNA-seq); (8) the ability to simultaneously track different types of cell in the same milieu; (9) the ability to measure migration at single-cell resolution and take into account cell heterogeneity; (10) what in vivo situation or process the in vitro assay best mimics (Supplementary Fig. 1); and (11) the number of cells needed to run the assay and perform post-assay molecular analysis, if applicable. A summary of the above criteria of selection for a cell migration assay is provided in Table 1.

Owing to the lack of practical guidelines, these different cell migration assays are often used interchangeably. This is despite that these assays are designed to mimic and understand sometimes completely different migratory processes. This and the inherent dynamic nature of migration, which often requires sophisticated live-cell microscopy, may have caused cell migration to be notably less well understood than equally important cell functions, such as cell differentiation or proliferation, for which 'black-box' end points (for example, plate readers and western blots) may be sufficient. Accordingly, in fixed tissues, there is often a poor correlation between apparent molecular markers of cell migration, such as those determined through pathway analysis[29], and actual cell migration itself, which may have limited the translation of mechanistic insights of cell migration into clinical treatments and companion diagnostics.

In this Review, we provide a comprehensive practical guide on how to choose, implement and use migration assays and how to best match that assay to the biological question at hand. We also provide a decision tree to help users decide the assay to use for their cell migration application (Supplementary Fig. 9). In a companion paper[30], we provide a comprehensive review of how to analyze the raw data generated by these different migration assays. We hope these guidelines will help newcomers to the field of cell migration to select the best assay to help address their biological question. We note that 'cell migration' and 'cell motility' are often used interchangeably in the literature to refer to cellular movement. For consistency, we will only use the word migration and reserve the word motility for the movement of subcellular organelles, such as endocytic vesicles[31] and the nucleus[32–34].

Assays to measure cell migration in vitro

Below, we describe ten standard (commercial) and advanced (custom) cell migration in vitro assays.

The wound healing assay (scratch assay)

The wound healing assay measures how a confluent monolayer of cells moves into a 'wound'[35,36] (Fig. 2). A 'wound' is introduced by scratching the confluent cell monolayer, which is then imaged frequently to study wound closure. Alternatively, commercially available obstacle stoppers can be used to exclude cells from a specific area, obviating the need

https://doi.org/10.1038/s41592-025-02890-1

Table 1 | Comparison of different in vitro migration assays

	Wound healing	Transwell	2D cell migration	3D cell migration	Spheroids/ organoids	Microslide chemotaxis	Confined migration	Micropattern migration
Dimensionality	2D	2.5D/3D	2D	3D	3D	2.5D	1D	1D
Throughput[a] (duration of the assay)	5 conditions 8–18 h	96 multiwell 16–48 h (depending on coating, pore size)	4–64 multiwell (motorized stage) 2–24 h (slow, fast cells)	4–64 wells (motorized stage) 2–24 h (slow, fast cells)	96 multiwell Multiple days	3 slots per assay 3–48 h (slow, fast cells)	10 conditions min–hours	10 conditions hours
Ease of implementation	Easy	Easy (commercial)	Easy	Difficult	Difficult	Easy (commercial)	Difficult	Difficult
Cost	Low	Medium (if use ECM)	Medium (if use ECM)	High (large amount of ECM)	High (large amount of ECM)	High (device)	Medium (custom PDMS)	Medium (custom PDMS)
Commercial availability	✓	✓	✗	✗	✗	✓	✗	✗
Productive capacity	High	High	Medium	Medium	Medium	High	High	Low
Live-cell microscopy	Not needed	Not needed	Needed	Needed	Needed	Needed	Needed	Needed
Post-assay downstream molecular analysis	✓	✗	✓	✓	✓	✗	✗	✗
Tracking at single-cell resolution (measure cell heterogeneity)	✗	✗	✓	✓	✓	✓	✓	✓
Incorporate different types of cell simultaneously	✗	✗	Cell tagging necessary	Cell tagging necessary	Cell tagging necessary	✗	✗	✗
Best mimic of in vivo scenario	Collective cell migration of epithelial or cancer cell sheets	Chemotactic or invasive cell migration through ECM fiber pores	Single-cell migration on flat substrates	Migration of individual cells in 3D matrix	Collective migration of cells in physiological 3D tumor microenvironment	Chemotaxis of individual cells	Confined migration	Migration of cells exposed to environmental geometries
Suitable cell types	Adherent	Adherent and suspension	Adherent	Adherent and suspension	Adherent and suspension	Adherent and suspension	Adherent and suspension	Adherent
Number of cells needed	Cells grow into desired confluency	~10^5 per cm^2 depending on insert size	~10^3–10^5 per well depending on well size, tech repeats are needed	~10^3–10^5 per gel depending on well size, tech repeats are needed	~10^4–10^5 per spheroid for cancer cells or stromal cells	~10^4 per channel (seed in observation area), tech repeats are needed	~10^5 per cell-seeding inlet	~10^4 per cm^2 depending on micropattern area
Advantages	Easy and cost-effective	Easy and cost-effective	Permits deeper analysis of migration via assessment of multiple migration parameters	Permits deeper analysis of migration, more physiologically relevant	Permits deeper analysis of migration, more physiologically relevant	Permits studying chemotaxis	Permits studying confined migration	Permits studying migration on custom-made patterns
Drawbacks	Affected by proliferation	Affected by proliferation	Requires live-cell tracking setup	Requires live-cell tracking setup and 3D culture ECM and reagents	Requires 3D culture ECM and reagents	Requires special chemotaxis slides	Requires specially fabricated slides	Requires specially fabricated slides

[a]Throughput is per experimental run.

to create a wound. Cell migration is characterized by calculating the diminishing percentage of the cell-free area at different time points until wound closure is reached or by simply recording time-lapsed videos to analyze leading-edge migration speed (Fig. 2; see the companion paper[30] for analysis of data from the assay). Although often used for mesenchymal cells such as fibroblasts and immune cells, it is more physiologically suited for epithelial cells[37,38], and is standard to investigate collective cell sheet migration[39–41]. The same principle can be used in the opposite manner, using fence assays[42,43]. Fence assays consist of restricting the initial seeding and adhesion of cells to a defined area, typically circular, before removing the restraint[42–44]. Outward cell migration into the cell-free region is then measured as with the scratch wound assay. In contrast to the traditional scratch assay, physical damage to the cells and the ECM is largely avoided.

Experimental setup. Cells are seeded on tissue culture plates and grown to confluency. A wound is introduced by making a scratch on the cell monolayer with a pipette tip[45,46] or by seeding cells confined to a specific area covered by lab-made or commercially available obstacle stoppers, typically made of silicone, in a well[47,48]. Coating the plate

https://doi.org/10.1038/s41592-025-02890-1

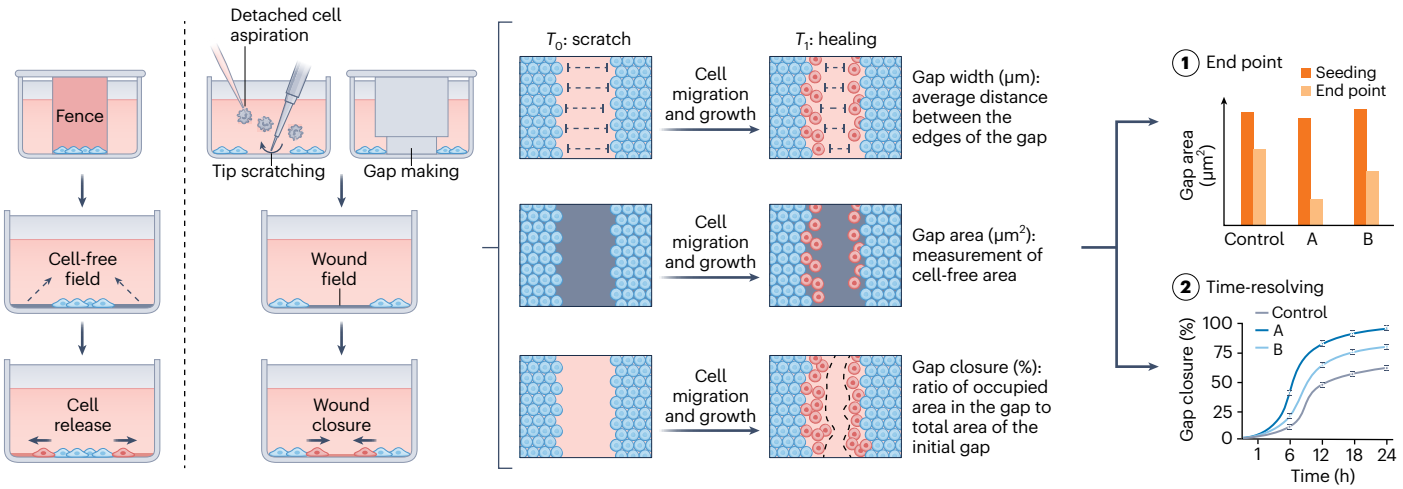

Fig. 2 | The wound healing assay. Tip scratching on the cell monolayer and applying obstacle stopper while seeding are the two common methods to introduce a cell-free 'wounded' field onto the tissue culture surface. In a fence assay, cells confined initially within a silicone insert can move into a cell-free 'empty' field after removal of the insert. For the scratch assay, from the scratch time T_0 to healing time point T_1, collective cell migration (and cell proliferation) contributes to the closure of the 'wounded' gap, which can be quantitatively assessed via measuring gap width or area and percentage of gap closure. Data analysis can be carried out either in the form of an end point, where gap areas from different conditions are measured at the same time point, or in a time-dependent manner, where gap closure is monitored and plotted against time for different conditions (see companion paper[30]). Figure created in BioRender.com. Du, F. (2025) https://BioRender.com/32bqvj0.

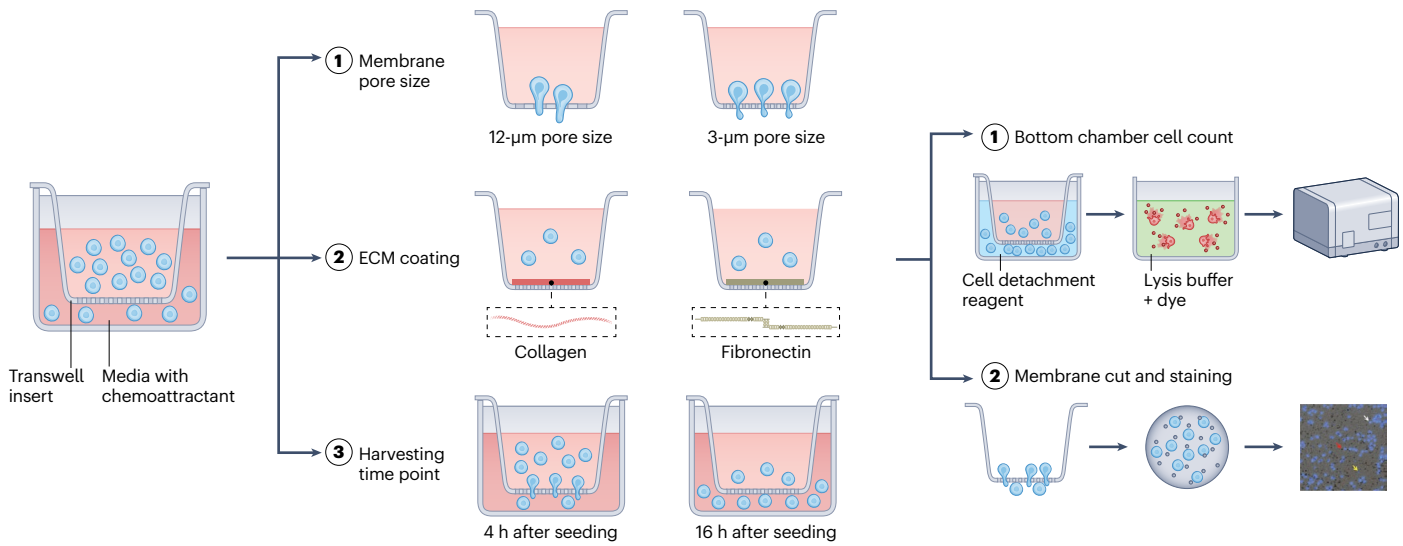

Fig. 3 | The Transwell assay (Boyden chamber assay). In a Transwell assay, cells are seeded into the insert chamber, which contains a porous membrane, while chemoattractant or conditioned medium is introduced in the bottom chamber, prompting the cells to migrate through the membrane. Modifications include different membrane pore size (for example, smaller-pore-sized membranes are more suitable for immune cells), ECM coating (for example, collagen or fibronectin coating for suspension cells expressing different types of adhesion molecule) and harvesting time point. Data acquisition can be carried out by cell counting in the bottom chamber (direct counting of the cells in the bottom chamber/indirect fluorescence-based cell lysis) or membrane staining via hematoxylin or specific antibodies (see companion paper[30]). Figure created in BioRender.com. Du, F. (2025) https://BioRender.com/2wjfz7j.

surface with an ECM-like collagen I, fibronectin or basal membrane extracts (Matrigel) makes it possible to study collective cell migration on substrates of different ECM compositions. Cells can also be cultured on engineered ECM-coated substrates of different stiffness (for example, polyacrylamide gels) to study the role of mechanosensing on collective cell migration[5]. Thanks to the 2D nature of the wound healing assay, it can be mounted on a light microscope for high-resolution imaging using high-magnification lenses (>×40) and glass coverslips. Standard phase-contrast or differential interference contrast microscopy can be used to track the leading edge of the cell monolayer moving into the wound (Table 1 and Fig. 2).

Advantages and limitations. The wound healing assay is convenient as it requires standard tissue culture plates, is the most technically straightforward among cell migration assays and is relatively cheap. A wound healing assay conducted over long periods of time—on the order of a day or more—cannot distinguish the contributions of cell proliferation and cell migration to wound closure and, with increased cell density resulting from proliferation, it becomes difficult to efficiently track individual cells. Another limitation is that the ECM coating can be inadvertently scraped off while making the wound, leading to uneven ECM coating, which can introduce artifacts (Table 1). This limitation can be overcome using the obstacle stoppers mentioned above[47,48]. The wound healing

https://doi.org/10.1038/s41592-025-02890-1

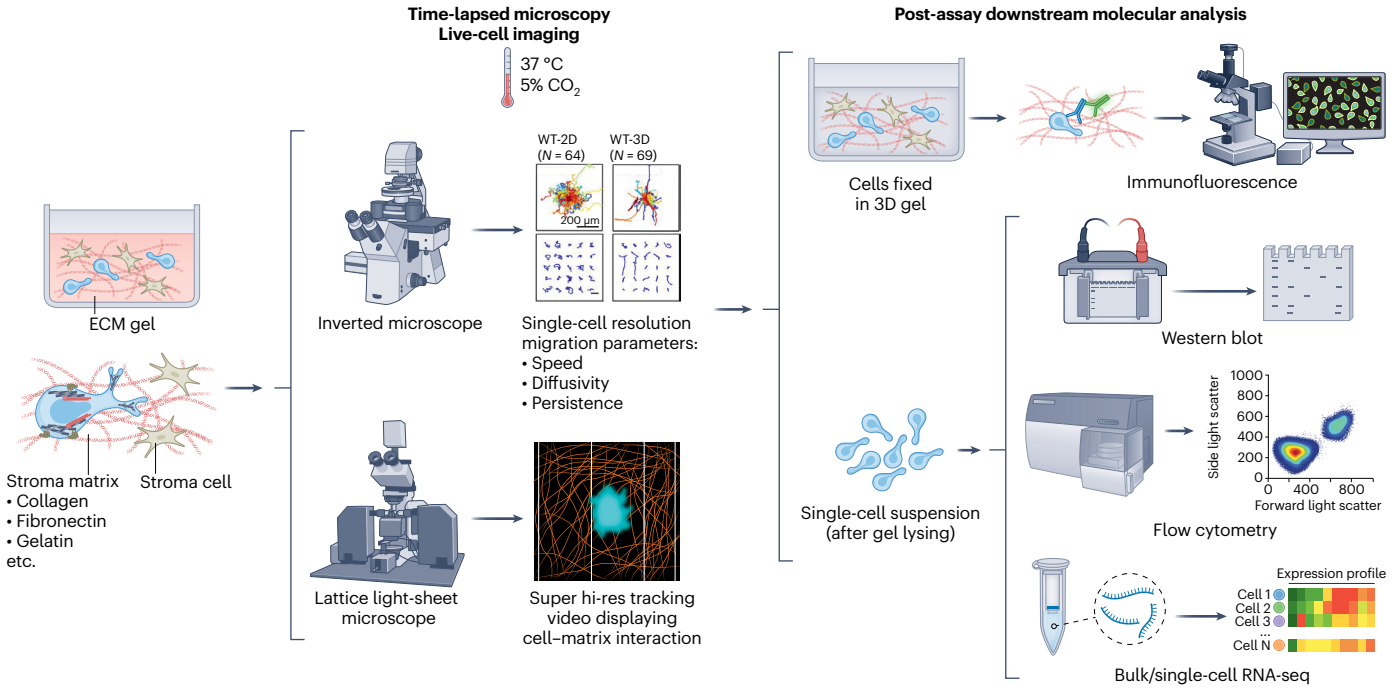

Fig. 4 | The 3D cell migration assay. Cells are embedded in an ECM matrix. Different ECM proteins (collagen, fibronectin, gelatin) are chosen according to the biological question. For setting up time-lapsed microscopy, live-cell conditions of 37 °C with 5% CO_2 are required. A traditional inverted microscope with phase-contrast or differential interference contrast lenses can be used to record videos for the characterization of migration parameters such as speed, diffusivity and persistence. If a high-resolution tracking video is required for a migration dynamics study, lattice light-sheet microscopy should be chosen for fast (sub-second) tracking. Cells embedded in 3D gels can be fixed and stained for immunofluorescence or used for post-assay downstream molecular analysis. For western blot, flow cytometry and bulk/single-cell RNA-seq, cells need to be lysed out from the gel and purifed (Table 1). Cell trajectories (middle) are reproduced from ref. 61, PNAS. Figure created in BioRender.com. Du, F. (2025) https://BioRender.com/yt2m0b6.

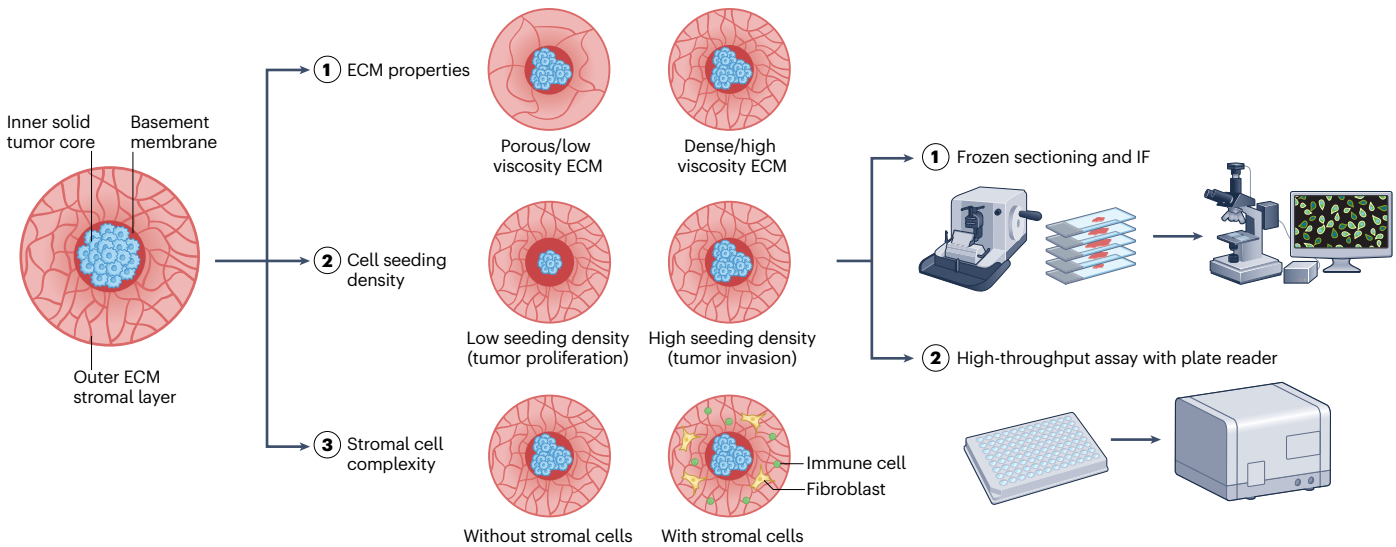

Fig. 5 | The spheroid/organoid invasion assay. In a multilayered spheroid setup, tumor cells are embedded in an inner core consisting of basement membrane extracts such as Matrigel to mimic the solid tumor core. An additional outer stromal layer made from common ECM proteins such as collagen I is wrapped around the tumor core to provide an invasion and migration space for investigating tumor proliferation and following metastasis, respectively. Tuning the collagen concentration in the outer layer results in modifications of porosity and visco-elasticity. The initial seeding density of tumor cells in the inner core can be chosen to reflect different tumor progression stages, either early-stage hyper-proliferation or later initialization of tumor invasion. Stromal cells that actively remodel the tumor microenvironment, including fibroblasts and immune cells, can be added into the outer layer. Similarly to tumor tissues, spheroids/organoids can be frozen or formalin fixed and paraffin embedded and sectioned to investigate cell migration at a single-cell spatial resolution. Mid-throughput analysis based on fluorescence using a plate reader is also feasible (Table 1). IF, immunofluorescence. Figure created in BioRender.com. Du, F. (2025) https://BioRender.com/w7xwlmc.

assay is relatively low throughout, which limits its use for genetic or pharmacological screens (Table 1; see also the perspective below).

The Transwell assay (Boyden chamber assay)

In a Transwell assay, also known as the Boyden chamber assay, cells are plated on one side of a porous membrane while a chemoattractant is introduced on the other side, prompting the cells to migrate through the membrane via chemotaxis[36,49,50] (Fig. 3). The essential principle of a Transwell assay lies in the capability of cells placed in the upper chamber to squeeze through this porous membrane made of polycarbonate/polyester under the influence of a chemoattractive gradient. Pores of different sizes and different incubation times can be tuned for different cell types, including cells of different size or different migratory potential[44]. Under most circumstances, smaller pore sizes (3–5 µm) are adopted for assessing the transmigration of lymphocytes and leukocytes[51,52], which allows for relative easy passage of small, adhesion-independent, amoeboid-like immune cells without overestimation of their migration rates due to passive diffusion driven by gravity, while larger pore size of 8–12 µm are used for adherent cancer and epithelial cells[53]. Large pores may be beneficial in reducing mechanical stress and thus ensuring better cell viability but they allow nonspecific migration, leading to false-positive results. Small pores introduce more confinement that requires more effort from cells to deform or degrade the ECM, reflecting more accurate invasive and migratory potential. Transwell assays can also be used to study molecular mechanisms of constricted/confined migration by having the cells squeeze through membranes with small pores[54–56].

Experimental setup. The setup is prepared by placing the Transwell inserts into the wells and adding culture medium containing cytokines to the outer compartment. Cells are detached (if adherent), counted and seeded by adding the cell suspension to the cell culture inserts. This setup is then placed in the incubator until the determined end point. At the end point, the membrane is fixed and nonmigratory cells remaining on the top side of the membrane can be wiped out using a cotton swab. The cells that have migrated onto the bottom side are stained with cytological dyes such as hematoxylin/crystal violet for counting purposes[53,57,58] or antibodies for immunofluorescence imaging[59,60] (see more details in the companion paper[30]). Control experiments consist of placing chemokines/cytokines in both the upper and bottom chambers or adding no cytokines. Other versions of the basic Transwell assay include coating the porous membrane with Matrigel to study mechanisms of cancer cell invasion or immune cell infiltration or placing a monolayer of endothelial cells to mimic cell extravasation or intravasation[53]. Cells seeded in the upper cell reservoir sink onto the Matrigel-coated porous membrane and the endothelial cell monolayer to form adhesion, where they then sense the higher concentration of chemokines/cytokines in the lower conditioned medium chamber to initiate chemotactic migration via ECM degradation together with paracellular/transcellular diapedesis (Table 1 and Fig. 3).

Advantages and limitations. The relative ease of use—there is no need for time-lapsed microscopy—and commercial availability from multiple suppliers (Corning, Thermo Fisher Scientific, BD), as well as the ability to study confined migration and the possibility to incorporate different ECMs, all account for the popularity of the Transwell assay. Nevertheless, the lack of easy post-assay molecular assessment due to the low number of migrated cells along with the non-negligible gravity-driven migration constitute major limitations of this assay. Similarly to the wound healing assay, proliferation can complicate the interpretation of the Transwell assay results (Table 1).

2D/3D single-cell migration assay

Even non-diseased clonal cells can have highly heterogeneous migratory properties, which are not recognized by the above assays (Table 1). These cellular heterogeneities are reflected in differences in migration parameters, including speed, diffusivity, persistence and anisotropy[61,62] (see Fig. 2 in the companion paper[30]). Cell speed measures the migratory capacity of a cell; it can only be computed if the movements of cells can be well fitted by a model of migration, such as the random-walk model[61]. Diffusivity is a parameter that also measures the migratory potential of cells but is model independent. The displacement of cells will also depend on how often cells change direction, which is measured by the cell persistence and anisotropy[61]. These parameters provide a more in-depth view of any change in cell migration caused by cell manipulations or changing microenvironments (see more details in the companion paper[30]). Computing these cell migration parameters requires the establishment of migration assays that track individual cells without the confounding effect of cell proliferation.

Experimental setup. Cells can be either seeded on an ECM-coated plate to analyze 2D migration or embedded inside a 3D ECM matrix and subjected to live-cell microscopy (Table 1 and Supplementary Fig. 4). To compute migration parameters in both geometries, cells need to be seeded at a sufficiently low density to minimize cellular collisions, and the duration of video recording needs to be approximately shorter than the cell doubling time[61,62] (see the companion paper[30] for details). While preparing gels, it is essential to solidify the gels as soon as possible to prevent cells from sinking to the bottom due to gravity, which makes cell distribution in the gel non-uniform. The robustness of the results is increased by tracking a sufficiently large number of cells[63] (Table 1).

Tracking can be automated by the assistance of open-source tracking algorithms[64,65] (see the companion paper[30]). Users should use resolutions and lenses of magnifications that fit their purpose, for instance, using a low-magnification lens (for example, ×10 or even lower) allows to record videos of migrating cells over a larger field of view. This boosts the number of tracked cells and reduces issues of cells coming in and out of the plane of focus during video capture, but at the expense of losing cell morphological details. Using lenses of higher magnification reduces the number of tracked cells, but allows to simultaneously extract migration and morphological information such as protrusion and nucleus dynamics from videos. Users should also use a frame rate based on the speed of the cells (Supplementary Table 1) and the number of conditions (that is, number of wells used in a multiwell device) to be probed. This choice is a compromise between a sufficiently high sampling rate based on cell speed to obtain enough statistics to properly extract migration parameters from model fits (see the companion paper[30]) and a sufficiently low sampling rate to be able to monitor cell migration in many wells at the same time and produce multiple videos simultaneously. Additionally, while analyzing overnight tracking videos, dividing cells must be excluded, which can be done manually or automatically via tracking software. Cells undergoing division will typically display lower migration, while cells finishing cytokinesis may display enhanced migration when they complete division, which may hinder analysis of pure migratory potential of the cells under study (Table 1).

Choosing between 2D and 3D. Although the 2D cell migration assay can mimic epithelial cell sheet migration on ECM substrates, in many cases cell migration across rigid and planar substrates cannot match the physiological context to be studied, such as the 3D architecture of the ECM and associated local fiber alignment and pore size of the tumor stromal matrix[17,66,67]. Consequently, higher biological significance has been attached to 3D cell migration assays where cells either are embedded in or invade an ECM gel mixture[20,68,69]. The most abundant ECM protein in the biological process or structure to be studied—for instance collagen I to study cancer cell migration in the tumor stromal matrix—should be chosen as the main component for the 3D gel. The effect of pharmacological treatments or conditioned medium

harvested from another cell culture can be introduced via addition on top of the gel. Unlike chemotaxis assays, the 3D cell migration assay focuses on the random (basal) migration of cells[5]. Video-based fluorescence microscopy of fluorescently labeled cells offers ease of tracking, while phase-contrast microscopy allows to record and analyze cell migration without cell labeling[61,70]. ECM fiber network remodeling and stress fields caused by cell movements and local MMP-based digestion and more detailed cellular dynamics can be assessed by reflection confocal microscopy[71–73] and lattice light-sheet microscopy[74,75], respectively. If the movements of the cells are isotropic (which is true if the mean displacements of the cells along the main orthogonal axes of the plane of focus are equal), then one can omit the measurements of the cells in the vertical direction. This circumvents the need for a computer-controlled microscope stage and cuts down on the size of the videos (Table 1 and Fig. 4).

Limitations. Although single-cell migration assays provide a lot more information about cell migration than end-point assessments, such as wound healing and Boyden chamber assays, they necessitate expensive environmental chambers to maintain cells at physiological temperature and CO_2 content. Additionally, imaging cells fully embedded in a 3D gel far from the walls of the cell culture well at high magnification or high resolution is difficult, if not impossible. Finally, post-assay molecular assessments such as western blots and RNA-seq require an additional gel digesting step to collect the cells (for example, using collagenase for collagen I matrices), as opposed to simple cell detachment from 2D plates (Table 1). For many types of cell such as stromal cells (for example, fibroblasts and immune cells), studying 3D cell migration is more physiologically relevant than 2D migration. However, the higher complexity and associated challenges with implementation—such as the large amount and associated higher cost of ECM required to make 3D gels—have hindered its popularity.

The spheroid/organoid invasion assay

Unlike stromal cells such as fibroblasts and immune cells, most solid tumors contain highly packed cancer cells. Three-dimensional spheroids/organoids can help measure and develop treatments to target cancer cell migration and invasion in 3D settings[76–79] (Fig. 5). Upon seeding onto an ultralow-adhesion surface followed by embedding into a 3D scaffolding matrix dome such as Matrigel, tissue-derived human tumor cells can grow into self-organizing organotypic structures called organoids[80], which are widely used in cancer research, including biomarker discovery[81], identifying molecular pathways driving tumor progression and guiding the development of anti-metastatic drugs[82]. Conventional tumor organoid cultures can only incorporate one ECM protein at a time, typically Matrigel[83,84], collagen[85] or synthetic hydrogels[86,87]. However, under most circumstances, the proliferation and invasion of cancer cells occurs in different ECM compartments—predominantly proliferation with little invasion/migration inside the basement membrane (Matrigel) and predominantly invasion with little proliferation in the collagen-rich stroma area.

Experimental setup. If cells are adherent, they are gently detached and centrifuged to pellet them[88], then resuspended in Matrigel on ice at a predetermined density. A small volume (~50 µl) of the resulting mix is added to the center of the well to make Matrigel 'domes'; the plate is placed in an incubator at 37 °C to solidify the Matrigel. Appropriate medium is added and the plate is returned to the incubator. Over time, the cells will proliferate to form organoids, which are imaged regularly to study cell migration and invasion.

Multilayered spheroids. Recently, oil-in-water droplet microtechnology has been utilized to produce multilayered co-culture spheroids with great structural consistency[89,90]. The inner spheroid core is made by suspending tumor cells in cold (liquid) Matrigel followed by incubation at 37 °C to solidify the Matrigel. This step allows to tune the seeding density of tumor cells in the core to study different scenarios, such as early hyper-proliferation or later-stage metastasis. This core is embedded in an outer collagen layer (corona) in which cancer-associated fibroblasts[91,92] and immune cells can be incorporated to study their roles in tumor progression. This multilayered organoid/spheroid system allows for high levels of consistency, versatility and correlation with in vivo models, while being high throughput (Table 1 and Fig. 5).

Limitations. Although commercially available low-adhesion plates greatly facilitate the 'streamlined' production of organoids/spheroids, the high cost of ECM proteins and relatively challenging protocols have prevented many from utilizing this 3D cell migration assay.

The microslide chemotaxis assay

Since the Transwell assay presents limitations, the horizontal double-chamber setting of microslides (µ-slides) has become more widely adopted to study chemotactic cell migration[93–95], especially for immune cells[96–98] (Supplementary Fig. 6). Examples of immune cell types studied using the µ-slide chemotaxis assay and their associated migration speed are provided in Supplementary Table 1.

Experimental setup. In a µ-slide, two large reservoirs are connected by a capillary, which also serves as the observation area. Cells are first seeded into the capillary on a 2D ECM-coated surface or in 3D ECM matrices[99,100] by pipetting cell suspensions in injection ports on either side of the observation area[101]. Fresh medium is added in one reservoir and conditioned medium containing potential chemokines (such as epidermal growth factor for cancer cells and macrophages, vascular endothelial growth factor for endothelial cells, CCL2 for monocytes and memory T cells, CCL17 for type 2 helper T cells and CXCL8 for neutrophils) in the other through the corresponding injection ports. A stable concentration gradient develops in the middle capillary area after incubation and time-lapse microscopy collects single-cell trajectories for directionality analysis (Supplementary Fig. 6). This gradient persists for up to 48 h[101].

Advantages and limitations. µ-Slides are commercially available from manufacturers such as ibidi and are well suited for screening chemotactic soluble factors or drugs. In addition to its simple setup, advantages include the low cell number requirement for seeding the observation area and the ability to perform up to three conditions simultaneously in one slide. However, other assays such as 2D/3D single-cell migration, scratch wound and Transwell assays are better fits for high-throughput screening compared to µ-slides (Table 1).

The confined migration assay

Besides the biochemical properties of the stromal matrix, its physical properties—such as pore size[102,103], visco-elasticity[104,105], viscosity[18] and osmotic pressure[106]—are also critical in influencing cell migration, both in vitro and in vivo[104,107]. Even for in vitro systems such as collagen and Matrigel gels, which are widely used as simplified models for 3D cell migration, it is challenging to control their physical properties so that the contribution of each parameter to cell migration can be estimated.

Experimental setup. To assess migration through a set pore size, microfabricated polydimethylsiloxane (PDMS) channel/micropattern devices with ECM-coated walls or ECM gel embedded are designed as a 1D confined migration assay[19,108] (Supplementary Fig. 7). Cells are seeded at a predetermined cell density and imaged. Owing to the confined nature of the cell migration behavior in these devices, leading and trailing edges of cells are more easily defined, enabling live tracking of dynamic actin assembly and other essential cytoskeleton networks[109,110].

Advantages and limitations. Simplified 1D cell tracking has facilitated the discovery of new mechanisms of cell migration, such as the water osmotic engine model[111,112]. Dedicated micropattern designs of these devices provide platforms for either high-throughput screening of potent chemotactic factors identified from conditioned media[113] or discovering decision-making cellular behaviors under intricated environments incorporated with multiple intersections for different paths[114,115]. The ability to study these properties/mechanisms is unique to these microfluidic devices. However, these devices are more expensive than the abovementioned assays (Table 1).

Migration on 2D micropatterns

Cells can also acquire a directional migration phenotype and bias their motion in response to geometric cues[116,117]. Two-dimensional micropattern systems are designed to impose asymmetric microgeometries as a guide for cell polarization and thus work as an alternative method to study directional cell migration[118] (Supplementary Fig. 8). Micropatterns can provide a dynamic, complex and micrometer-scale habitat for cell migration induced by different protein substrate shapes. The most common micropattern formation protocol was originally introduced by Bernard et al. in 1998 as microcontact printing technique[119], in which adhesive proteins such as fibronectin or laminin are equilibrated on the surface of micropattern mold (for most of the cases PDMS) and transferred with high efficiency to substrates such as plastic and glass[120,121]. With advancement in biomedical device microfabrication, newer methods such as extrusion-based 3D printing[122] and meniscus-dragging deposition plus photolithography[123] have also been developed for more complicated micropattern designs.

Experimental setup. Seeded cells attached to functionalized 2D adhesive regions are tracked via light microscopy and video recording to characterize the directional migration of cells on either single-cell or collective levels[124].

Limitations. Considering the limited paths that cells can choose for migration, the 2D micropattern migration assay of cells is more akin to 1D confined migration with limited readouts of cell migration such as speed and probability of entry. The relatively small amount of ECM proteins printed on the micropattern surface is prone to alterations by cell-mediated degradation and cells secreting their own ECM. The printed patterns also limit throughput because only very few cells can be tracked and thus limiting downstream molecular assessments such as transcriptomics or proteomics (Table 1).

Assays to measure cell migration in vivo

Although major advances have been achieved in the development of various in vitro and ex vivo methods, to investigate cell migration and decipher the corresponding downstream signaling pathways, even the most advanced 3D matrix cell migration and multi-compartment spheroid systems often fail to mimic the full complexity and dynamics of the cellular microenvironment encountered in living tissues, such as anatomical compartmentalization and hydrodynamic forces of fluid flow. Intravital microscopy (IVM) is now playing an indispensable role in in vivo cell migration measurements[125], among which multi-photon[126–128] and light-sheet microscopies are the most widely adopted. With accumulated progress in fluorescence labeling and light microscopy, IVM has expanded the field of in vivo live-cell tracking by enabling greater depths, extended observation windows, larger tissue areas and more refined subcellular resolutions.

Live-cell tracking via multi-photon microscopy

Conventional confocal microscopy can generate volumetric images of 3D samples by separating signals of planes of interest from the noise coming from out-of-focus signals[129]. Nevertheless, limited penetration capability to excite fluorescence in the tissue of interest restricts the application of confocal microscopy to intravital cell migration assay. Deep sectioning is made possible by taking advantage of the underlying principle that excitation in multi-photon microscopy arises from the simultaneous absorption of two or three photons in a single quantized event[130]. Owing to the longer wavelength required for multi-photon microscopy, red and infrared lasers are used, which reduce scattering compared to conventional microscopy.

In general, techniques that are more advanced come at the expense of higher complexity and cost of setup. Surprisingly, this is not the case for multi-photon microscopy, as setting it up is not much different than conventional microscopy. However, IVM requires suitable mouse models and associated complex surgeries[131]. In vivo endogenous tagging of specific cell types (for example, different immune cells) can be achieved by cross-breeding commercially available transgenic reporter mouse stains[132]. Ex vivo cell staining (live-cell tracker dye such as CFDA-SE, green; CMTPX, red) before adoptive transfer can also be incorporated together with tagged fluorescent proteins to provide great contrast in the observation window area[133]. Genetically encoded fluorescent proteins coupled with different labeling probes enable the tracking of more than one cell population, and cellular heterogeneity is taken into account via single-cell tracking.

Phototoxicity is a crucial challenge in multi-photon IVM owing to the need for high laser intensity to penetrate deep into live tissues[134,135]. Even with increased laser intensity, visualization depths using the widely adopted skin window chamber model or the skull bone marrow model remains limited to 100–300 μm[136]. High peak power laser pulses can generate reactive oxygen species, leading to oxidative stress, cell damage and tissue inflammation, together with localized heating, which alters cell physiology[137]. To mitigate photocytotoxicity, high signal-to-noise ratio and photostable imaging probes for cell labeling such as quantum dots and carbon dots probes[138,139] that do not require high excitation levels and are excited at longer wavelengths should be used, together with supplementation of antioxidants (reactive oxygen species scavengers) such as ascorbic acid[140], trolox[141,142] and flavonoids[143]. For imaging, pulse modulation including the pulse gating implementation[144] and dispersion compensation[145] could be applied to deliver excitation energy more efficiently without elongating exposure, which can further be coupled with recently developed deep-learning-based denoising methods to maintain imaging resolution and quality with a minimal dose of radiation[146,147]. Live-cell tracking at organ level can be set up via surgical procedures in which organs are exteriorized and superfused with saline solution, at a risk of inflammatory reactions. The high difficulty of implementation makes it impossible to reach higher throughput like more convenient in vitro counterparts.

Cell tracking in whole organisms via light-sheet microscopy

Light-sheet microscopy allows to visualize and quantitatively monitor dynamic biological processes in vivo at high spatiotemporal resolution[148], from the movements of single molecules in a cell to the movements of cells in whole organisms[74,149–154]. Unlike widefield and confocal microscopy, which both illuminate the entire thickness of the specimen, light-sheet microscopy uses a separate excitation lens perpendicular to the detection lens so that illumination is confined to the focal plane[148]. Whereas conventional light sheets are created with Gaussian beams that are too thick for subcellular dimensions, lattice light-sheet microscopy using updated 2D optical lattices as the illumination source has been developed more recently for hyper-speed (sub-second) 4D live-cell tracking of intercellular or cell–matrix interaction[74,75].

Similarly to multi-photon microscopy, light-sheet microscopy requires appropriate labeling for different target cell types to track more than one cell population, which increases the difficulty of implementation. Additionally, its application is still relatively limited to embryogenesis of transparent organisms for living imaging, leaving its capability for organ-level deep sectioning yet to be shown.

How to select a cell migration assay

The selection of a migration assay requires the consideration of several factors, such as the type of migration to be studied (Supplementary Figs. 1–5), the equipment available and its cost (Table 1 and Fig. 1), the importance of potential confounding effects of cell proliferation (Table 1) and the type of downstream molecular assays to be performed (Table 1). In general, it is better to assess migration and validate results via two separate techniques, especially if those techniques have complementary strengths, for example, Transwell + organoids, which together permit migration assessments in 2D and 3D systems, or a single-cell migration assay + organoids, which allow for single-cell tracking and end-point analysis.

Use of Table 1, which lists many possible considerations, could suffice for the selection of the most appropriate assay for a given cell migration study. An alternative is the use of decision trees. Supplementary Fig. 9 shows a decision tree to select the most appropriate cell migration assay when the requirement for live-cell microscopy is the primary consideration. Other decision trees are possible when the primary consideration is instead dimensionality (say 1D versus 2D versus 3D), commercial availability, throughput or the need to measure cell migration heterogeneity. In the present case, the first consideration is whether live-cell tracking is necessary. Live-cell tracking allows for deeper analysis of cell migration by allowing for the computation of migration parameters such as velocity, diffusivity, persistence time and persistence speed, as well as quantify the heterogeneity of migration. Assays that allow for live-cell imaging also allow for live mechanism tracking/temporal analysis if the protein of interest is fluorescently tagged. However, live-cell tracking requires equipment such as live-cell boxes and microscopes capable of automated overnight imaging. Live-cell imaging can also be applied to the nonrandom walk types of migration described above such as chemotaxis, confined migration and migration on micropatterned substrates. In the absence of live-cell imaging equipment, end-point analysis will have to suffice. However, the absence of live-cell tracking makes it difficult to dissociate proliferation from migration. Differences in proliferation can influence results of wound healing or Transwell assays, whereas with live-cell tracking, dividing cells are easily excluded from analysis. In our example (Supplementary Fig. 9), the second consideration is the dimensionality of the assay (Supplementary Fig. 4) and the type of ECM to be used, with 3D assays being preferable to 2D assays owing to their greater physiological relevance. Each assay can use a different ECM to better mimic different biological processes, for example, migration through a stromal matrix or invasion through a basement membrane. Following the previous two decision-making steps, the third consideration finalizes the choice of selected migration assay on the basis of whether information about cellular heterogeneity should be provided or not.

The above considerations (for example, the use of microfluidics, necessity for live-cell tracking, ECM coatings) lead to a more comprehensive analysis of migration and/or better mimicking of in vivo systems. However, their incorporation leads to more expensive and labor-intensive experimental setups. Hence, assays such as wound healing and Transwell can provide an easy, quick and inexpensive assessment of cell migration. All assays mentioned are well suited for adherent cells. Some 2D assays, for example, scratch wound assay and 2D live-cell tracking, may need ECM coating to study migration of suspension cells, such as T cells and B cells. Other factors can be tuned for each assay such as the incorporation of multiple cell types in a single assay (for example, Figs. 3 and 5) and the type of mechanistic assays to be conducted downstream. The incorporation of multiple cell types allows us to study the influence of other cell types, such as immune cells and cancer-associated fibroblasts, on cancer cells and vice versa. To track multiple cell types, each type of cell type must be labeled either by endogenous expression of fluorescent proteins or by staining with dyes mentioned in the section (Table 1). For situations where the cells of interest cannot be labeled, conditioned medium from the other cells can be used as a preliminary and approximate way to mimic the presence of those cells. The assays mentioned above (except for microfluidics-based assays and assays requiring fixation such as Transwell) are also conducive to downstream mechanistic analysis at the DNA/epigenetic, RNA and protein levels via standard techniques such as PCR, RNA-seq, western blotting, immunofluorescence and flow cytometry. The assays need to be scaled up accordingly to yield the number of cells required for the downstream analysis of interest. For assays in which it is difficult to harvest enough cells for downstream analysis, it is recommended to plate cells for both sets of experiments simultaneously. This reduces errors that arise from batch-to-batch variations (biological replicates) and ensures that any mechanisms determined would be done in cells whose migration have been simultaneously investigated.

The companion paper[30] provides an in-depth review of the analytical and computational methods required to analyze the data generated by the above cell migration assays.

Outlook

Despite the central role that cell migration has in health and disease, cell migration assays are still a long way from being widely adopted owing to their (sometimes necessary) complexity, cost and low throughput. We anticipate that cell migration assays will see the following technological advances in the next few years:

1. As none of the above cell migration assays is truly high throughput, throughput needs to be increased to test, for instance, 1,000–10,000s of candidate inhibitors/activators of cell migration per run. This would require technological advances in device automation and new AI-based software for the reliable and automatic tracking of millions of cells. Such high-throughput assays would open the door to much larger short hairpin RNA/small interfering RNA/CRISPR/drug screens to gain new mechanistic insights and discover new regulators of cell migration.
2. To identify molecular determinants of migratory heterogeneities, new methods need to be developed to functionally connect single-cell migration measurements to single-cell transcriptomic/proteomic profiles in the same combined assay. This would identify putative molecular drivers of migratory behaviors across biological contexts. For instance, the confined migration assay could be extended to collect individual cells from each channel for downstream molecular characterization.
3. Considerably larger in vitro and in vivo cell migration datasets tightly connected to transcriptomic data are needed to produce more reliable gene signatures of different modes of cell migration. Robust cell migration signatures would greatly help distinguish, for instance, migratory versus nonmigratory cells in tissue sections via spatial transcriptomic mapping. These large datasets would require high temporal resolution and long recording times to evaluate the effect of temporal resolution on the magnitude of cell migration features. These datasets would be used to build models to harmonize datasets across different laboratories and identify the ideal temporal resolution given experimental constraints, such as the number of conditions, cell types, and so on.

Reporting summary

Further information on research design is available in the Nature Portfolio Reporting Summary linked to this article.

References

1. Keller, R. Cell migration during gastrulation. *Curr. Opin. Cell Biol.* **17**, 533–541 (2005).
2. Chuai, M., Hughes, D. & Weijer, C. J. Collective epithelial and mesenchymal cell migration during gastrulation. *Curr. Genomics* **13**, 267–277 (2012).

3. Fu, X. et al. Mesenchymal stem cell migration and tissue repair. *Cells* **8**, 784 (2019).
4. Wirtz, D., Konstantopoulos, K. & Searson, P. C. The physics of cancer: the role of physical interactions and mechanical forces in metastasis. *Nat. Rev. Cancer* **11**, 512–522 (2011).
5. Du, W., Nair, P., Johnston, A., Wu, P. -H. & Wirtz, D. Cell trafficking at the intersection of the tumor–immune compartments. *Annu. Rev. Biomed. Eng.* **24**, 275–305 (2022).
6. Friedl, P. & Gilmour, D. Collective cell migration in morphogenesis, regeneration and cancer. *Nat. Rev. Mol. Cell Biol.* **10**, 445–457 (2009).
7. Jain, S. et al. The role of single-cell mechanical behaviour and polarity in driving collective cell migration. *Nat. Phys.* **16**, 802–809 (2020).
8. Sherratt, J. A. Chemotaxis and chemokinesis in eukaryotic cells: the keller-segel equations as an approximation to a detailed model. *Bull. Math. Biol.* **56**, 129–146 (1994).
9. Shellard, A. & Mayor, R. Durotaxis: the hard path from in vitro to in vivo. *Dev. Cell* **56**, 227–239 (2021).
10. Rens, E. G. & Merks, R. M. H. Cell shape and durotaxis explained from cell-extracellular matrix forces and focal adhesion dynamics. *iScience* **23**, 101488 (2020).
11. Gruler, H. & Nuccitelli, R. Neural crest cell galvanotaxis: new data and a novel approach to the analysis of both galvanotaxis and chemotaxis. *Cell Motil. Cytoskeleton* **19**, 121–133 (1991).
12. Huang, Y. -J. et al. Cellular microenvironment modulates the galvanotaxis of brain tumor initiating cells. *Sci. Rep.* **6**, 21583 (2016).
13. Goswami, P. et al. Magnetotactic bacteria and magnetofossils: ecology, evolution and environmental implications. *NPJ Biofilms Microbiomes* **8**, 43 (2022).
14. Gardel, M. L., Schneider, I. C., Aratyn-Schaus, Y. & Waterman, C. M. Mechanical integration of actin and adhesion dynamics in cell migration. *Annu. Rev. Cell Dev. Biol.* **26**, 315–333 (2010).
15. Yamaguchi, H. & Condeelis, J. Regulation of the actin cytoskeleton in cancer cell migration and invasion. *Biochim. Biophys. Acta* **1773**, 642–652 (2007).
16. Vicente-Manzanares, M., Ma, X., Adelstein, R. S. & Horwitz, A. R. Non-muscle myosin II takes centre stage in cell adhesion and migration. *Nat. Rev. Mol. Cell Biol.* **10**, 778–790 (2009).
17. Yamada, K. M. & Sixt, M. Mechanisms of 3D cell migration. *Nat. Rev. Mol. Cell Biol.* **20**, 738–752 (2019).
18. Bera, K. et al. Extracellular fluid viscosity enhances cell migration and cancer dissemination. *Nature* **611**, 365–373 (2022).
19. Paul, C. D., Hung, W. C., Wirtz, D. & Konstantopoulos, K. Engineered models of confined cell migration. *Annu. Rev. Biomed. Eng.* **18**, 159–180 (2016).
20. Lämmermann, T. et al. Rapid leukocyte migration by integrin-independent flowing and squeezing. *Nature* **453**, 51–55 (2008).
21. Lämmermann, T. & Sixt, M. Mechanical modes of 'amoeboid' cell migration. *Curr. Opin. Cell Biol.* **21**, 636–644 (2009).
22. Wolf, K. et al. Compensation mechanism in tumor cell migration: mesenchymal–amoeboid transition after blocking of pericellular proteolysis. *J. Cell Biol.* **160**, 267–277 (2003).
23. Marcadis, A. R. et al. Rapid cancer cell perineural invasion utilizes amoeboid migration. *Proc. Natl Acad. Sci. USA* **120**, e2210735120 (2023).
24. Paňková, K., Rösel, D., Novotný, M. & Brábek, J. The molecular mechanisms of transition between mesenchymal and amoeboid invasiveness in tumor cells. *Cell. Mol. Life Sci.* **67**, 63–71 (2010).
25. Loza, A. J. et al. Cell density and actomyosin contractility control the organization of migrating collectives within an epithelium. *Mol. Biol. Cell* **27**, 3459–3470 (2016).
26. Tlili, S. et al. Collective cell migration without proliferation: density determines cell velocity and wave velocity. *R. Soc. Open Sci.* **5**, 172421 (2018).
27. Kalluri, R. & Weinberg, R. A. The basics of epithelial-mesenchymal transition. *J. Clin. Invest.* **119**, 1420–1428 (2009).
28. Dongre, A. & Weinberg, R. A. New insights into the mechanisms of epithelial–mesenchymal transition and implications for cancer. *Nat. Rev. Mol. Cell Biol.* **20**, 69–84 (2019).
29. Nair, P. R. et al. MLL1 regulates cytokine-driven cell migration and metastasis. *Sci. Adv.* **10**, eadk0785 (2024).
30. Wu, P. H. et al. Methods to analyze cell migration data: fundamentals and practical guidelines. *Nat. Methods* https://doi.org/10.1038/s41592-025-02935-5 (2025).
31. Bananis, E., Murray, J. W., Stockert, R. J., Satir, P. & Wolkoff, A. W. Regulation of early endocytic vesicle motility and fission in a reconstituted system. *J. Cell Sci.* **116**, 2749–2761 (2003).
32. Kiss, A., Horvath, P., Rothballer, A., Kutay, U. & Csucs, G. Nuclear motility in glioma cells reveals a cell-line dependent role of various cytoskeletal components. *PLoS ONE* **9**, e93431 (2014).
33. Morris, N. R. Nuclear migration. From fungi to the mammalian brain. *J. Cell Biol.* **148**, 1097–1101 (2000).
34. Lee, J. S., Chang, M. I., Tseng, Y. & Wirtz, D. Cdc42 mediates nucleus movement and MTOC polarization in Swiss 3T3 fibroblasts under mechanical shear stress. *Mol. Biol. Cell* **16**, 871–880 (2005).
35. Jonkman, J. E. N. et al. An introduction to the wound healing assay using live-cell microscopy. *Cell Adh. Migr.* **8**, 440–451 (2014).
36. Hulkower, K. I. & Herber, R. L. Cell migration and invasion assays as tools for drug discovery. *Pharmaceutics* **3**, 107–124 (2011).
37. Alard, A. et al. Breast cancer cell mesenchymal transition and metastasis directed by DAP5/eIF3d-mediated selective mRNA translation. *Cell Rep.* **42**, 112646 (2023).
38. Shimizu, T. et al. Indigo enhances wound healing activity of Caco-2 cells via activation of the aryl hydrocarbon receptor. *J. Nat. Med.* **75**, 833–839 (2021).
39. Kim, J. H. et al. Propulsion and navigation within the advancing monolayer sheet. *Nat. Mater.* **12**, 856–863 (2013).
40. Simpson, K. J. et al. Identification of genes that regulate epithelial cell migration using an siRNA screening approach. *Nat. Cell Biol.* **10**, 1027–1038 (2008).
41. Chapnick, D. A. & Liu, X. Leader cell positioning drives wound-directed collective migration in TGFβ-stimulated epithelial sheets. *Mol. Biol. Cell* **25**, 1586–1593 (2014).
42. Das, A. M., Eggermont, A. M. M. & ten Hagen, T. L. M. A ring barrier–based migration assay to assess cell migration in vitro. *Nat. Protoc.* **10**, 904–915 (2015).
43. Wager, L. J., Murray, R. Z., Thompson, E. W. & Leavesley, D. I. A fence barrier method of leading edge cell capture for explorative biochemical research. *Cell Adh. Migr.* **11**, 496–503 (2017).
44. Kramer, N. et al. In vitro cell migration and invasion assays. *Mutat. Res.* **752**, 10–24 (2013).
45. Yarrow, J. C., Perlman, Z. E., Westwood, N. J. & Mitchison, T. J. A high-throughput cell migration assay using scratch wound healing, a comparison of image-based readout methods. *BMC Biotechnol.* **4**, 21 (2004).
46. Kam, Y., Guess, C., Estrada, L., Weidow, B. & Quaranta, V. A novel circular invasion assay mimics in vivo invasive behavior of cancer cell lines and distinguishes single-cell motility in vitro. *BMC Cancer* **8**, 198 (2008).
47. Acosta, S., Canclini, L., Galarraga, C., Justet, C. & Alem, D. Lab-made 3D printed stoppers as high-throughput cell migration screening tool. *SLAS Technol.* **27**, 39–43 (2022).
48. Cappiello, F., Casciaro, B. & Mangoni, M. L. A novel in vitro wound healing assay to evaluate cell migration. *J. Vis. Exp.* 17, 56825 (2018).

49. Boyden, S. The chemotactic effect of mixtures of antibody and antigen on polymorphonuclear leucocytes. *J. Exp. Med.* **115**, 453–466 (1962).
50. Albini, A. et al. A rapid in vitro assay for quantitating the invasive potential of tumor cells. *Cancer Res.* **47**, 3239–3245 (1987).
51. Oner, A. & Kobold, S. Transwell migration assay to interrogate human CAR-T cell chemotaxis. *STAR Protoc.* **3**, 101708 (2022).
52. Knieke, K. et al. CD152 (CTLA-4) determines CD4 T cell migration in vitro and in vivo. *PLoS ONE* **4**, e5702 (2009).
53. Albini, A. & Benelli, R. The chemoinvasion assay: a method to assess tumor and endothelial cell invasion and its modulation. *Nat. Protoc.* **2**, 504–511 (2007).
54. Pfeifer, C. R. et al. Constricted migration increases DNA damage and independently represses cell cycle. *Mol. Biol. Cell* **29**, 1948–1962 (2018).
55. Xia, Y. et al. Rescue of DNA damage after constricted migration reveals a mechano-regulated threshold for cell cycle. *J. Cell Biol.* **218**, 2545–2563 (2019).
56. Jacobson, E. C. et al. Migration through a small pore disrupts inactive chromatin organization in neutrophil-like cells. *BMC Biol.* **16**, 142 (2018).
57. Zhang, F. et al. Astrocyte elevated gene-1 interacts with β-catenin and increases migration and invasion of colorectal carcinoma. *Mol. Carcinog.* **52**, 603–610 (2013).
58. Tang, C. L. et al. Focal adhesion kinase signaling is necessary for the cyclosporin A-enhanced migration and invasion of human trophoblast cells. *Placenta* **33**, 704–711 (2012).
59. Gillespie, J. L., Anyah, A., Taylor, J. M., Marlin, J. W. & Taylor, T. A. A versatile method for immunofluorescent staining of cells cultured on permeable membrane inserts. *Med. Sci. Monit. Basic Res.* **22**, 91–94 (2016).
60. Kreiseder, B. et al. α-Catulin downregulates E-cadherin and promotes melanoma progression and invasion. *Int. J. Cancer* **132**, 521–530 (2013).
61. Wu, P. -H., Giri, A., Sun, S. X. & Wirtz, D. Three-dimensional cell migration does not follow a random walk. *Proc. Natl Acad. Sci. USA* **111**, 3949–3954 (2014).
62. Wu, P. -H., Giri, A. & Wirtz, D. Statistical analysis of cell migration in 3D using the anisotropic persistent random walk model. *Nat. Protoc.* **10**, 517–527 (2015).
63. Gómez-de-Mariscal, E. et al. Use of the p-values as a size-dependent function to address practical differences when analyzing large datasets. *Sci. Rep.* **11**, 20942 (2021).
64. Hilsenbeck, O. et al. Software tools for single-cell tracking and quantification of cellular and molecular properties. *Nat. Biotechnol.* **34**, 703–706 (2016).
65. Jaqaman, K. et al. Robust single-particle tracking in live-cell time-lapse sequences. *Nat. Methods* **5**, 695–702 (2008).
66. Wu, P. -H., Gilkes, D. M. & Wirtz, D. The biophysics of 3D cell migration. *Annu. Rev. Biophys.* **47**, 549–567 (2016).
67. Konstantopoulos, K., Wu, P. H. & Wirtz, D. Dimensional control of cancer cell migration. *Biophys. J.* **104**, 279–280 (2013).
68. Zaman, M. H. et al. Migration of tumor cells in 3D matrices is governed by matrix stiffness along with cell-matrix adhesion and proteolysis. *Proc. Natl Acad. Sci. USA* **103**, 10889–10894 (2006).
69. Fraley, S. I., Feng, Y., Giri, A., Longmore, G. D. & Wirtz, D. Dimensional and temporal controls of three-dimensional cell migration by zyxin and binding partners. *Nat. Commun.* **3**, 719 (2012).
70. Phillip, J. M. et al. Fractional re-distribution among cell motility states during ageing. *Commun. Biol.* **4**, 81 (2021).
71. Guilbert, M. et al. Highlighting the impact of aging on type I collagen: label-free investigation using confocal reflectance microscopy and diffuse reflectance spectroscopy in 3D matrix model. *Oncotarget* **7**, 8546–8555 (2016).
72. Maska, M. et al. Quantification of the 3D collagen network geometry in confocal reflection microscopy. In *2015 IEEE International Conference on Image Processing (ICIP)* 1791–1794 (IEEE, Quebec City, 2015).
73. Steinwachs, J. et al. Three-dimensional force microscopy of cells in biopolymer networks. *Nat. Methods* **13**, 171–176 (2016).
74. Chen, B. -C. et al. Lattice light-sheet microscopy: imaging molecules to embryos at high spatiotemporal resolution. *Science* **346**, 1257998 (2014).
75. Fritz-Laylin, L. K. et al. Actin-based protrusions of migrating neutrophils are intrinsically lamellar and facilitate direction changes. *eLife* **6**, e26990 (2017).
76. Zhao, Z. et al. Organoids. *Nat. Rev. Methods Primers* **2**, 94 (2022).
77. Drost, J. & Clevers, H. Organoids in cancer research. *Nat. Rev. Cancer* **18**, 407–418 (2018).
78. LeSavage, B. L., Suhar, R. A., Broguiere, N., Lutolf, M. P. & Heilshorn, S. C. Next-generation cancer organoids. *Nat. Mater.* **21**, 143–159 (2022).
79. Costa, E. C. et al. 3D tumor spheroids: an overview on the tools and techniques used for their analysis. *Biotechnol. Adv.* **34**, 1427–1441 (2016).
80. Hofer, M. & Lutolf, M. P. Engineering organoids. *Nat. Rev. Mater.* **6**, 402–420 (2021).
81. Verduin, M., Hoeben, A., De Ruysscher, D. & Vooijs, M. Patient-derived cancer organoids as predictors of treatment response. *Front. Oncol.* **11**, 641980 (2021).
82. Veninga, V. & Voest, E. E. Tumor organoids: opportunities and challenges to guide precision medicine. *Cancer Cell* **39**, 1190–1201 (2021).
83. Takebe, T. et al. Vascularized and functional human liver from an iPSC-derived organ bud transplant. *Nature* **499**, 481–484 (2013).
84. Broutier, L. et al. Culture and establishment of self-renewing human and mouse adult liver and pancreas 3D organoids and their genetic manipulation. *Nat. Protoc.* **11**, 1724–1743 (2016).
85. Ootani, A. et al. Sustained in vitro intestinal epithelial culture within a Wnt-dependent stem cell niche. *Nat. Med.* **15**, 701–706 (2009).
86. Gjorevski, N. et al. Designer matrices for intestinal stem cell and organoid culture. *Nature* **539**, 560–564 (2016).
87. Hernandez-Gordillo, V. et al. Fully synthetic matrices for in vitro culture of primary human intestinal enteroids and endometrial organoids. *Biomaterials* **254**, 120125 (2020).
88. Zhang, S., Cheng, G., Zhu, S., Lin, D. & Wu, C. Protocol for the generation, characterization, and functional assays of organoid cultures from normal and cancer-prone human esophageal tissues. *STAR Protoc.* **5**, 103316 (2024).
89. Russo, G. C. et al. E-cadherin interacts with EGFR resulting in hyper-activation of ERK in multiple models of breast cancer. *Oncogene* **43**, 1445–1462 (2024).
90. Lee, M. -H. et al. Multi-compartment tumor organoids. *Mater. Today* **61**, 104–116 (2022).
91. Nakamura, H. et al. Organoid culture containing cancer cells and stromal cells reveals that podoplanin-positive cancer-associated fibroblasts enhance proliferation of lung cancer cells. *Lung Cancer* **134**, 100–107 (2019).
92. Tsai, S. et al. Development of primary human pancreatic cancer organoids, matched stromal and immune cells and 3D tumor microenvironment models. *BMC Cancer* **18**, 335 (2018).
93. Tomasova, L., Guttenberg, Z., Hoffmann, B. & Merkel, R. Advanced 2D/3D cell migration assay for faster evaluation of chemotaxis of slow-moving cells. *PLoS ONE* **14**, e0219708 (2019).
94. Grognot, M. & Taute, K. M. A multiscale 3D chemotaxis assay reveals bacterial navigation mechanisms. *Commun. Biol.* **4**, 669 (2021).

95. Cockx, M. et al. Neutrophils from patients with primary ciliary dyskinesia display reduced chemotaxis to CXCR2 ligands. *Front. Immunol.* **8**, 1126 (2017).
96. Kamakura, S. et al. The cell polarity protein mInsc regulates neutrophil chemotaxis via a noncanonical G protein signaling pathway. *Dev. Cell* **26**, 292–302 (2013).
97. Larasati, R. A. et al. The role of butyrate on monocyte migration and inflammation response in patient with type 2 diabetes mellitus. *Biomedicines* **7**, 74 (2019).
98. Chakrabarti, J. et al. Sonic hedgehog acts as a macrophage chemoattractant during gastric epithelial regeneration in response to injury. *FASEB J.* **33**, 869.827 (2019).
99. Huang, Y. et al. Three-dimensional hydrogel is suitable for targeted investigation of amoeboid migration of glioma cells. *Mol. Med. Rep.* **17**, 250–256 (2018).
100. Pepperell, E. E. & Watt, S. M. A novel application for a 3-dimensional timelapse assay that distinguishes chemotactic from chemokinetic responses of hematopoietic CD133$^+$ stem/progenitor cells. *Stem Cell Res.* **11**, 707–720 (2013).
101. Zengel, P. et al. μ-Slide chemotaxis: a new chamber for long-term chemotaxis studies. *BMC Cell Biol.* **12**, 21 (2011).
102. Tien, J. et al. Matrix pore size governs escape of human breast cancer cells from a microtumor to an empty cavity. *iScience* **23**, 101673 (2020).
103. Wolf, K. et al. Physical limits of cell migration: control by ECM space and nuclear deformation and tuning by proteolysis and traction force. *J. Cell Biol.* **201**, 1069–1084 (2013).
104. Charras, G. & Sahai, E. Physical influences of the extracellular environment on cell migration. *Nat. Rev. Mol. Cell Biol.* **15**, 813–824 (2014).
105. Doyle, A. D., Carvajal, N., Jin, A., Matsumoto, K. & Yamada, K. M. Local 3D matrix microenvironment regulates cell migration through spatiotemporal dynamics of contractility-dependent adhesions. *Nat. Commun.* **6**, 8720 (2015).
106. Miermont, A., Lee, S. W. L., Adriani, G. & Kamm, R. D. Quantitative screening of the effects of hyper-osmotic stress on cancer cells cultured in 2- or 3-dimensional settings. *Sci. Rep.* **9**, 13782 (2019).
107. Paul, C. D., Mistriotis, P. & Konstantopoulos, K. Cancer cell motility: lessons from migration in confined spaces. *Nat. Rev. Cancer* **17**, 131–140 (2017).
108. Holle, A. W. et al. Cancer cells invade confined microchannels via a self-directed mesenchymal-to-amoeboid transition. *Nano Lett.* **19**, 2280–2290 (2019).
109. Tong, Z. et al. Chemotaxis of cell populations through confined spaces at single-cell resolution. *PLoS ONE* **7**, e29211 (2012).
110. Hung, W. C. et al. Confinement sensing and signal optimization via piezo1/PKA and myosin II pathways. *Cell Rep.* **15**, 1430–1441 (2016).
111. Stroka, K. M. et al. Water permeation drives tumor cell migration in confined microenvironments. *Cell* **157**, 611–623 (2014).
112. Li, Y., Yao, L., Mori, Y. & Sun, S. X. On the energy efficiency of cell migration in diverse physical environments. *Proc. Natl Acad. Sci. USA* **116**, 23894–23900 (2019).
113. Yang, Z. et al. High throughput confined migration microfluidic device for drug screening. *Small* **19**, 2207194 (2023).
114. Zanotelli, M. R. et al. Energetic costs regulated by cell mechanics and confinement are predictive of migration path during decision-making. *Nat. Commun.* **10**, 4185 (2019).
115. Zhao, R. et al. Cell sensing and decision-making in confinement: the role of TRPM7 in a tug of war between hydraulic pressure and cross-sectional area. *Sci. Adv.* **5**, eaaw7243 (2019).
116. Vedula, S. R. K. et al. Emerging modes of collective cell migration induced by geometrical constraints. *Proc. Natl Acad. Sci. USA* **109**, 12974–12979 (2012).
117. Jiang, X., Bruzewicz, D. A., Wong, A. P., Piel, M. & Whitesides, G. M. Directing cell migration with asymmetric micropatterns. *Proc. Natl Acad. Sci. USA* **102**, 975–978 (2005).
118. Fink, A. et al. Area and geometry dependence of cell migration in asymmetric two-state micropatterns. *Biophys. J.* **118**, 552–564 (2020).
119. Bernard, A. et al. Printing patterns of proteins. *Langmuir* **14**, 2225–2229 (1998).
120. Chen, C. S., Mrksich, M., Huang, S., Whitesides, G. M. & Ingber, D. E. Micropatterned surfaces for control of cell shape, position, and function. *Biotechnol. Prog.* **14**, 356–363 (1998).
121. Fink, J. et al. Comparative study and improvement of current cell micro-patterning techniques. *Lab Chip* **7**, 672–680 (2007).
122. Du, W., Hong, S., Scapin, G., Goulard, M. & Shah, D. I. Directed collective cell migration using three-dimensional bioprinted micropatterns on thermoresponsive surfaces for myotube formation. *ACS Biomater. Sci. Eng.* **5**, 3935–3943 (2019).
123. Kim, S. E. et al. Cell migration according to shape of graphene oxide micropatterns. *Micromachines* **7**, 186 (2016).
124. Mahmud, G. et al. Directing cell motions on micropatterned ratchets. *Nat. Phys.* **5**, 606–612 (2009).
125. Pittet, M. J. & Weissleder, R. Intravital imaging. *Cell* **147**, 983–991 (2011).
126. Flesken-Nikitin, A., Williams, R. M., Zipfel, W. R., Webb, W. W. & Nikitin, A. Y. Use of multiphoton imaging for studying cell migration in the mouse. *Methods Mol. Biol.* **294**, 335–345 (2005).
127. Kedrin, D., Wyckoff, J., Sahai, E., Condeelis, J. & Segall, J. E. Imaging tumor cell movement in vivo. *Curr. Protoc. Cell Biol.* **19**, Unit 19.17 (2007).
128. Supatto, W., McMahon, A., Fraser, S. E. & Stathopoulos, A. Quantitative imaging of collective cell migration during *Drosophila* gastrulation: multiphoton microscopy and computational analysis. *Nat. Protoc.* **4**, 1397–1412 (2009).
129. Lucas, L., Gilbert, N., Ploton, D. & Bonnet, N. Visualization of volume data in confocal microscopy: comparison and improvements of volume rendering methods. *J. Microsc.* **181**, 238–252 (1996).
130. Hoover, E. E. & Squier, J. A. Advances in multiphoton microscopy technology. *Nat. Photonics* **7**, 93–101 (2013).
131. Sahai, E. et al. Simultaneous imaging of GFP, CFP and collagen in tumors in vivo using multiphoton microscopy. *BMC Biotechnol.* **5**, 14 (2005).
132. Jain, R. et al. Visualizing murine breast and melanoma tumor microenvironment using intravital multiphoton microscopy. *STAR Protoc.* **2**, 100722 (2021).
133. Miller, M. J., Wei, S. H., Cahalan, M. D. & Parker, I. Autonomous T cell trafficking examined in vivo with intravital two-photon microscopy. *Proc. Natl Acad. Sci. USA* **100**, 2604–2609 (2003).
134. Benninger, R. K. P. & Piston, D. W. Two-photon excitation microscopy for the study of living cells and tissues. *Curr. Protoc. Cell Biol.* **4**, 4.11.1–4.11.24 (2013).
135. Svoboda, K. & Yasuda, R. Principles of two-photon excitation microscopy and its applications to neuroscience. *Neuron* **50**, 823–839 (2006).
136. Durr, N. J., Weisspfennig, C. T., Holfeld, B. A. & Ben-Yakar, A. Maximum imaging depth of two-photon autofluorescence microscopy in epithelial tissues. *J. Biomed. Opt.* **16**, 026008 (2011).
137. Kasprzycka, W., Szumigraj, W., Wachulak, P. & Trafny, E. A. New approaches for low phototoxicity imaging of living cells and tissues. *Bioessays* **46**, 2300122 (2024).
138. Hallaji, Z. et al. An insight into the potentials of carbon dots for in vitro live-cell imaging: recent progress, challenges, and prospects. *Mikrochim. Acta* **189**, 190 (2022).

139. Soha, S. A. et al. Improved imaging and preservation of lysosome dynamics using silver nanoparticle-enhanced fluorescence. *Mol. Biol. Cell* **34**, ar96 (2023).
140. Harada, T. et al. An antioxidant screen identifies ascorbic acid for prevention of light-induced mitotic prolongation in live cell imaging. *Commun. Biol.* **6**, 1107 (2023).
141. Seker, U. et al. Trolox is more successful than allopurinol to reduce degenerative effects of testicular ischemia/reperfusion injury in rats. *J. Pediatr. Urol.* **16**, 465.e461–465.e468 (2020).
142. Vorobjeva, N. V. & Pinegin, B. V. Effects of the antioxidants Trolox, Tiron and Tempol on neutrophil extracellular trap formation. *Immunobiology* **221**, 208–219 (2016).
143. Zahra, M., Abrahamse, H. & George, B. P. Flavonoids: antioxidant powerhouses and their role in nanomedicine. *Antioxidants* **13**, 922 (2024).
144. Song, J. et al. SNR enhanced high-speed two-photon microscopy using a pulse picker and time gating detection. *Sci. Rep.* **13**, 14244 (2023).
145. Pérez-Vizcaíno, J. et al. Dispersion management in two-photon microscopy by using diffractive optical elements. *Opt. Lett.* **38**, 440–442 (2013).
146. Guan, H. et al. Deep-learning two-photon fiberscopy for video-rate brain imaging in freely-behaving mice. *Nat. Commun.* **13**, 1534 (2022).
147. He, Y. et al. Self-supervised deep-learning two-photon microscopy. *Photon. Res.* **11**, 1–11 (2023).
148. Wan, Y., McDole, K. & Keller, P. J. Light-sheet microscopy and its potential for understanding developmental processes. *Annu. Rev. Cell Dev. Biol.* **35**, 655–681 (2019).
149. Lu, C. -H. et al. Lightsheet localization microscopy enables fast, large-scale, and three-dimensional super-resolution imaging. *Commun. Biol.* **2**, 177 (2019).
150. Kaur, P., Saunders, T. E. & Tolwinski, N. S. Coupling optogenetics and light-sheet microscopy, a method to study Wnt signaling during embryogenesis. *Sci. Rep.* **7**, 16636 (2017).
151. Weber, M. & Huisken, J. Light sheet microscopy for real-time developmental biology. *Curr. Opin. Genet. Dev.* **21**, 566–572 (2011).
152. Schmied, C. & Tomancak, P. Sample preparation and mounting of drosophila embryos for multiview light sheet microscopy. *Methods Mol. Biol.* **1478**, 189–202 (2016).
153. Khairy, K., Lemon, W. C., Amat, F. & Keller, P. J. Light sheet-based imaging and analysis of early embryogenesis in the fruit fly. *Methods Mol. Biol.* **1189**, 79–97 (2015).
154. Hillman, E. M. C., Voleti, V., Li, W. & Yu, H. Light-sheet microscopy in neuroscience. *Annu Rev. Neurosci.* **42**, 295–313 (2019).

Acknowledgements

We acknowledge the following sources of support: U54AR081774 (to D.W.), U54CA268083 (to D.W.), R01CA300052 (to D.W.), UG3CA275681 (to P.-H.W.) and UH3CA275681 (to P.-H.W.) all from the National Cancer Institute; and R35-GM157099 (to J.M.P.) from the National Institute of General Medical Sciences and the American Federation for Aging Research Glenn Foundation Junior Faculty Award (to J.M.P.).

Author contributions

D.W. conceived the outline. W.D., P.R.N., A.F., J.M.P., P.-H.W. and D.W. wrote the paper. W.D. produced the figures.

Competing interests

The authors declare no competing interests.

Additional information

Supplementary information The online version contains supplementary material available at https://doi.org/10.1038/s41592-025-02890-1.

Correspondence and requests for materials should be addressed to Jude M. Phillip, Pei-Hsun Wu or Denis Wirtz.

Peer review information *Nature Methods* thanks Li Yang, and the other, anonymous, reviewer(s) for their contribution to the peer review of this work. Primary Handling Editor: Rita Strack, in collaboration with the *Nature Methods* team.

nature portfolio

Corresponding author(s): Denis Wirtz

Last updated by author(s): Jul 7, 2025

Reporting Summary

Nature Portfolio wishes to improve the reproducibility of the work that we publish. This form provides structure for consistency and transparency in reporting. For further information on Nature Portfolio policies, see our Editorial Policies and the Editorial Policy Checklist.

Statistics

For all statistical analyses, confirm that the following items are present in the figure legend, table legend, main text, or Methods section.

n/a	Confirmed
☒	☐ The exact sample size (*n*) for each experimental group/condition, given as a discrete number and unit of measurement
☒	☐ A statement on whether measurements were taken from distinct samples or whether the same sample was measured repeatedly
☒	☐ The statistical test(s) used AND whether they are one- or two-sided *Only common tests should be described solely by name; describe more complex techniques in the Methods section.*
☒	☐ A description of all covariates tested
☒	☐ A description of any assumptions or corrections, such as tests of normality and adjustment for multiple comparisons
☒	☐ A full description of the statistical parameters including central tendency (e.g. means) or other basic estimates (e.g. regression coefficient) AND variation (e.g. standard deviation) or associated estimates of uncertainty (e.g. confidence intervals)
☒	☐ For null hypothesis testing, the test statistic (e.g. *F*, *t*, *r*) with confidence intervals, effect sizes, degrees of freedom and *P* value noted *Give P values as exact values whenever suitable.*
☒	☐ For Bayesian analysis, information on the choice of priors and Markov chain Monte Carlo settings
☒	☐ For hierarchical and complex designs, identification of the appropriate level for tests and full reporting of outcomes
☒	☐ Estimates of effect sizes (e.g. Cohen's *d*, Pearson's *r*), indicating how they were calculated

Our web collection on statistics for biologists contains articles on many of the points above.

Software and code

Policy information about availability of computer code

Data collection	Not Applicable
Data analysis	BioRender was used to generate all illustration figures in this review

For manuscripts utilizing custom algorithms or software that are central to the research but not yet described in published literature, software must be made available to editors and reviewers. We strongly encourage code deposition in a community repository (e.g. GitHub). See the Nature Portfolio guidelines for submitting code & software for further information.

Data

Policy information about availability of data

All manuscripts must include a data availability statement. This statement should provide the following information, where applicable:

- Accession codes, unique identifiers, or web links for publicly available datasets
- A description of any restrictions on data availability
- For clinical datasets or third party data, please ensure that the statement adheres to our policy

No new datasets were used in this review.

Human research participants

Policy information about studies involving human research participants and Sex and Gender in Research.

Reporting on sex and gender	Not Applicable
Population characteristics	Not Applicable
Recruitment	Not Applicable
Ethics oversight	Not Applicable

Note that full information on the approval of the study protocol must also be provided in the manuscript.

Field-specific reporting

Please select the one below that is the best fit for your research. If you are not sure, read the appropriate sections before making your selection.

☒ Life sciences ☐ Behavioural & social sciences ☐ Ecological, evolutionary & environmental sciences

For a reference copy of the document with all sections, see nature.com/documents/nr-reporting-summary-flat.pdf

Life sciences study design

All studies must disclose on these points even when the disclosure is negative.

Sample size	184 studies (research articles and reviews) were evaluated in a systematic review analysis.
Data exclusions	Studies that used migration assays were included (the majority of studies included were peer-reviewed; a few preprints were also included due to their significance). Studies were excluded when they were not primarily in English.
Replication	Not Applicable
Randomization	Not Applicable
Blinding	Not Applicable

Reporting for specific materials, systems and methods

We require information from authors about some types of materials, experimental systems and methods used in many studies. Here, indicate whether each material, system or method listed is relevant to your study. If you are not sure if a list item applies to your research, read the appropriate section before selecting a response.

Materials & experimental systems

n/a	Involved in the study
☒	☐ Antibodies
☒	☐ Eukaryotic cell lines
☒	☐ Palaeontology and archaeology
☒	☐ Animals and other organisms
☒	☐ Clinical data
☒	☐ Dual use research of concern

Methods

n/a	Involved in the study
☒	☐ ChIP-seq
☒	☐ Flow cytometry
☒	☐ MRI-based neuroimaging